Observation of lower hybrid drift instability in the diffusion region at a reconnecting magnetopause

S. D. Bale, F. S. Mozer, and T. Phan

Space Sciences Laboratory, University of California, Berkeley

Abstract. Intense lower hybrid waves are observed in the Hall current region of a reconnecting current sheet at the earth's magnetopause. Large measured cross-field drifts and density gradients are the likely sources of free energy through a lower hybrid drift instability (LHDI), which is stabilized near the neutral point where the plasma β is large. Harris neutral sheet and linear models are fitted to the data and inferred current density profiles are compared to the observed current density from particle measurements. We estimate the contribution of LHDI anomalous resistivity to the parallel electric field and show that it is more than 100 times smaller than the measured parallel field at the separator boundaries and essentially zero near the neutral point, leaving gradient electron pressure tensor and inertial terms or anomalous resistivity from higher frequency instabilities to support any parallel fields there and, hence, control the reconnection process.

1. Introduction

Magnetic reconnection proceeds when some process breaks the frozen-flux condition, embodied by the ideal MHD assumption of $\vec{E} + \vec{v} \times \vec{B} = 0$. This assumption can be broken by any of several terms in the generalized Ohm's law. In a collisionless plasma, one such term is ηj due to the anomalous resistivity of wave-particle interactions. Motivated by observations of noise in the lower-hybrid frequency range [e.g. *Gurnett et al.*, 1979; *Cattell et al.*, 1995], the lower hybrid drift instability (LHDI) has long been invoked as a possible source of anomalous resistivity in reconnecting current sheets [e.g. *Labelle and Treumann*, 1988; *Cattell et al.*, 1995]. LHDI is driven by cross-field drifts in the presence of density or magnetic field gradients; the growth rate peaks at $k\rho_e \approx 1$ for a broad range of frequencies near f_{LH}. The LHDI, however, ought to be stabilized at large β [*Davidson et al.*, 1977], a result that we show experimentally in this letter. This excludes the LHDI and any associated resistivity from near the neutral point, where reconnection onset is thought to occur. Recent laboratory reconnection experiments, in a different regime of collisionality, [*Carter et al.*, 2002a; *Carter et al.*, 2002b] show similar results, including the quenching of LHDI at the neutral point. This suggests that LHDI anomalous resistivity is not essential for reconnection. Our data indicates that this is also the case at the magnetopause.

The Polar spacecraft encountered a reconnection diffusion region at the magnetopause on April 1, 2001 near the subsolar point. The topology, flows, and reconnection rate of this event have been discussed by *Mozer et al.* [2002]. In this letter, we analyze observations of LHDI in the current sheet and show that the estimated contributions to plasma resistivity are negligible for the reconnection process.

Paper number .
0094-8276/02/$5.00

2. Observations and Analysis

Electric and magnetic field data, spacecraft potential, and electron and ion moments from the EFI, MFI, and Hydra experiments on Polar are used. Three-axis electric field measurements are sampled at 40 samples/s; magnetic field is sampled at 8.3 samples/s. The cadence of the ion and electrons moments is 1 per 13.8 sec and 1 per 4.6 sec respectively. These measurements are also discussed by *Mozer et al.* [2002]. The EFI axial electric field boom is short (13.6 m tip-to-tip) and the integrity of the measurement of small $E_\parallel$, which controls reconnection, requires a fortuitous orientation of the spacecraft with respect to the magnetic field. Spacecraft potential data is fitted locally to plasma density to produce an effective density measurement n_ϕ at high cadence (5 samples/s).

Figure 1 shows an overview of this event. Panel (d) shows the magnetic field vector in a minimum variance of B coordinate system. The transition from a southward magnetosheath ($B_z \approx$ -80 nT) field to northward magnetospheric ($B_z \approx$ 80 nT) field is easily seen in the maximum variance (red) component. The intermediate (green) component shows a clear example of the bipolar magnetic signature of a Hall current in the $\hat{y}$ direction. In panel (c), the measured electric field is shown in the Normal Incidence Frame (NIF) and in the same, minimum variance of B, coordinate system. The NIF is defined as a frame that moves along the magnetopause surface such that the incoming plasma flows in along the normal direction. The Hall current signatures again are clear in the normal component of the NIF electric field, while the tangential electric field is fairly constant indicating a steady state magnetopause ($\vec{\nabla} \times \vec{E} \approx 0$). An analysis of this tangential electric field gives a magnetopause speed of $v_{mp} \approx$ 24 km/s [*Mozer et al.*, 2002]. Wavelet spectrograms of $\vec{B}_{MV}$ and $\vec{E}_{NIF}$ are shown in panels (a) and (b) respectively; red lines on the spectrograms show the local ion cyclotron frequency f_{ci}, while the black line on panel (b) is the local lower hybrid resonance frequency $f_{lh} \approx (f_{ci} f_{ce})^{1/2}$. Noise above f_{ci} is visible in the electric spectrogram; its occurrence coincides spatially with the Hall current region. The magnetic and electric fluctuation spectrograms appear qualitatively different; while this may be a characteristic of the LHDI, it may also arise due to different sampling rates and instrument filters. Here, we focus on the electric field measurements. Wavelet power spectra (Figure 2) of the electric fluctuations show clear enhancements between f_{ci} and f_{lh}. The black and magenta spectra are sampled on the

magnetosheath (05:46:50-05:47:03 UT) and magnetosphere (05:47:11-05:47:22 UT) sides within the Hall current region, while the green spectrum is from the quiet magnetosphere (05:47:36-05:48:00 UT). Each spectrum is an average of several local spectra and has been binned in frequency scaled to f_{ci}. Heavy solid dots on each spectrum show where the Polar spacecraft spin frequency ($f_{spin} \approx 1/6$ Hz) occurs, which contaminates the spectrum. The quiet magnetosphere (green) and the Hall current regions below f_{ci} have spectra with similar slopes; the spectra in the Hall current region (red and magenta), however, show clear enhancements above ion cyclotron frequency and departures from the background power law. These spectra roll off near $20 f_{ci}$, just below f_{LH}; however, this may be an effect of the instrument low pass filters. A 7-pole low pass filter at the Nyquist frequency ($f_{ny} = 20$ Hz) prevents an accurate amplitude measurement near f_{ny} and the actual spectrum may not be attenuated near f_{LH} as observed. Broken power laws (dotted lines on the figure) fitted to the Hall current spectra give power law indices $\alpha_{1<} \approx -2.36$ ($f < f_{ci}$) and $\alpha_{1>} \approx -1.02$ ($f > f_{ci}$) for the magnetosheath side of the Hall current region (black spectrum). On the magnetosphere side (magenta), we get $\alpha_{2<} \approx -1.52$ and $\alpha_{2>} \approx -1.06$. A single power law fit gives an index of $\alpha_{mp} \approx -1.97$ in the quiet magnetosphere (green).

Electric fluctuations $\delta\vec{E}$ are calculated by detrending E_{NIF} using a 32-point (0.8 sec) running boxcar average and transforming to a magnetic field-aligned coordinate system (panel (a) of Figure 3). The polarization of the electric fluctuations is computed by doing a 32-point running maximum variance analysis on $\delta\vec{E}$. Panel (c) of Figure 3 shows the latitude of the maximum variance direction in field-aligned coordinate system and shows that the electric fluctuations are primarily perpendicularly polarized; the small polarization angle near the neutral point is unreliable, as the magnetic field direction may have a large error here. Ion plasma $\beta_i = 8\pi n k T_i / B^2$ is shown in panel (d), as calculated from the ion moment temperature, the effective density, and magnetic field. As $|B|$ goes to zero at the neutral point, β_i rises from its ambient value of approximately 0.1 to a peak of about 270. Red dotted, vertical lines in Figure 3 show the interval during which $\beta_i \geq 1$. This coincides with the damping of the electric fluctuations noted earlier, in agreement with prediction of LHDI. The density scale length $L_n = n/|dn/dx|$ in units of local electron inertial length c/ω_{pe} is shown in panel (b); as discussed above, the LHDI may be driven by large density gradients. Comparing panels (a) and (b) it can be seen that the most intense LHDI occurs when L_n is less than a few c/ω_{pe} and is quenched when $\beta_i >> 1$.

The transition from magnetosheath to magnetospheric magnetic field (panel (f) of Figure 3) is seen in B_z to have approximately the hyperbolic tangent profile of a Harris neutral sheet [*Harris*, 1962]. The black dotted line in panel (d) is a fit to B_0 tanh(x/L), where the best-fit parameters are $B_0 \approx 83.5$ nT and $L \approx 1.48\ c/\omega_{pi}$. For a generalized Harris sheet, $L = c/\omega_{ci}\sqrt{2}\ c_s/v_{drift}$, where c_s is the sound speed [e.g. *Yamada et al.*, 2000]. For this model, our fit gives $v_{drift} \approx c_s$, suggesting the possible growth of (unobserved) higher frequency electrostatic current-driven instabilities. A linear fit to B_z (red dotted line) gives $\partial B_z/\partial x \approx 35.3$ nT $(c/\omega_{pi})^{-1}$. Panel (e) shows the derived Harris sheet j_{HS} (black dotted line), linear j_L (red dotted line), and measured j_m (connected black dots) plasma current. The derived current j_{HS} is calculated from the derivative of the model field $\vec{j}_B = B_0/(\mu_0 L)\ \mathrm{sech}^2(x/L)\hat{y}$ and j_L is $1/\mu_0\ \partial B_z/\partial x$, while the measured current is computed from the difference of measured ion and electron velocity moments $\vec{j}_M = n_\phi e(\vec{u}_i - \vec{u}_e)$. Both model currents are larger than the observed current density near the center of the current sheet. The Harris sheet current profile agrees well with the measured current density near the edges.

We attempt to evaluate the contribution of anomalous resistivity to the physics in the current sheet. In the generalized Ohm's law, sources of parallel electric field may arise from ambipolar, inertial, and collisional physics $E_\parallel \approx \hat{B}\cdot[-(\vec{\nabla}\cdot\mathbf{P}_e)/en + (1/\epsilon_0\omega_{pe}^2)d\vec{j}/dt + \eta\vec{j}]$, where $\mathbf{P}$ is the electron pressure tensor and η is resistivity provided by collisions or wave-particle interactions. In the steady-state, ambipolar terms are thought to dominate; here we estimate the anomalous resistivity term $|\eta j|$ due to wave-particle interactions with the LHDI fields. Panel (a) of Figure 4 shows the absolute value of the measured parallel electric field $E_\parallel$. The direction cosine of the spacecraft spin plane and the local magnetic field is near zero here, therefore the magnetic field lies in the plane of the long, spin-plane electric field probes, minimizing the error in the measurement of $\vec{E}$: the large spike in $E_\parallel$ during a portion of the crossing near 05:47:20 is therefore well-measured. The perpendicular components of E are of the same magnitude here, but may be generated by Hall and convective terms in Ohm's law, hence we use $E_\parallel$ for comparison.

In the LH wave fields $\delta\vec{E}$, electrons may diffuse across field lines by their $\delta\vec{E}\times\vec{B}$ drift. *Coroniti* (1985) estimated the anomalous collision frequency between electrons and LH waves as $\nu_* \approx (\omega_{pe}^2/\omega_{lh})\epsilon_0\delta E^2/2nk_bT_e$. Using this expression, anomalous resistivity can be calculated as $\eta \approx \nu_*/(\epsilon_0\omega_{pe}^2)$ and the contribution to the electric field is $|\eta j|$ and is shown in panel (b) of Figure 4. While convection and Hall currents can have large contributions to the observed $E_\perp$, the physics of $E_\parallel$ is determined as above in Ohm's Law. The estimated ηj term follows the observed $E_\parallel$ near the separator boundaries; however, it is more than 100 times smaller in magnitude. Futhermore, since the LHDI is not observed near the neutral point, ηj is very small there and any contribution of the resistivity to anomalous diffusion will be small, as predicted by theory [e.g. *Coroniti*, 1985], whereas $E_\parallel$ is expected to remain finite near the neutral point [e.g. *Pritchett*, 2001].

3. Summary

We report observations of lower hybrid frequency fluctuations in the Hall current region of a reconnecting dayside magnetopause. The waves are intense, with $e\phi/k_bT_e \approx eE\rho_e/k_bT_e \approx 0.1$, perpendicularly polarized, and coincide spatially with the Hall current and a region of large density gradients. At the neutral point, where plasma β is large, the instability is quenched. Based on these properties, we identify the fluctuations as a lower hybrid drift instability (LHDI). We estimate that the contribution of anomalous resistivity, from the electric part of the fluctuations, to the observed DC electric field in the current sheet is small; hence any primary role in magnetic reconnection is unlikely. Two caveats are in order: the amplitude of the LHDI fluctuations may be underestimated due to instrument filter rolloff, in which case the actual anomalous resistivity can be larger. This is likely to be a small effect except just near the Nyquist frequency. On the other hand, recent simulations [*Watt et*

al., 2002] have shown that analytic estimates [e.g. *Labelle and Treumann*, 1988] of resistivity due to ion acoustic fluctuations may be several orders of magnitude too low. This could be the case for anomalous resistivity in LHDI turbulence as well, in which case our evaluation of ηj may be too small.

Acknowledgments. This work was supported by NASA grants NAG5-11733 and NAG5-11987 to the University of California. We thank J. D. Scudder and C. T. Russell for access to the Polar Hydra and MFI data, respectively.

References

Carter, T. A., et al., Measurement of lower-hybrid drift turbulence in a reconnecting current sheet, *Phys. Rev. Lett., 88*, 015001, 2002a.

Carter, T. A., et al., Experimental study of lower-hybrid drift turbulence in a reconnecting current sheet, *Phys. Plasmas*, *9*, 3272, 2002b.

Cattell, C. A., et al., ISEE 1 and Geotail observations of low-frequency waves at the magnetopause, *J. Geophys. Res., 100*, 11,823, 1995.

Coroniti, F., Space plasma turbulent dissipation: Reality or myth?, *Space Sci. Rev.*, *42*, 399, 1985.

Davidson, R. C., et al., Effects of finite plasma beta on the lower-hybrid-drift-instability, *Phys. Fluids*, *20*, 301, 1977.

Gurnett, D. A., et al., Plasma wave turbulence at the magnetopause: Observations from ISEE 1 and 2, *J. Geophys. Res., 84*, 7043, 1979.

Harris, E. G., *Nuovo Cimento*, *23*, 115, 1962.

Labelle, J. A., and R. Treumann, Plasma waves at the dayside magnetopause, *Space Sci. Rev.*, *47*, 175, 1988.

Mozer, F. S., S. D. Bale, and T. Phan, Observations of ion and electron diffusion regions at a sub-solar magnetopause reconnection event, *Phys. Rev. Lett., 89*, 015002, 2002.

Pritchett, P. L., Collisionless magnetic reconnection in a three-dimensional open system, *J. Geophys. Res., 106*, 25,961, 2001.

Watt, C. E., et al, Ion-acoustic resistivity in plasmas with similar ion and electron temperatures, *Geophys. Res. Lett.,* 29, 10.1029/2001GL013451, 2002.

Yamada, M., et al., Experimental investigation of the neutral sheet profile during magnetic reconnection, *Phys. Plasmas*, 7, 1781, 2000.

Stuart D. Bale, Forrest S. Mozer, and Tai Phan, Space Sciences Laboratory, University of California, Berkeley, CA 94720, USA (bale@ssl.berkeley.edu)

(Received _____.)

.

Figure 1. Overview of the magnetopause crossing from magnetosheath to magnetosphere. Spectrograms of magnetic (panel a) and electric (panel b) fluctuations show power in the Hall current regime (panels c and d). In particular, the electric fluctuations above f_{ci} (red line) are lower hybrid-like.

Figure 2. Wavelet power spectra of electric fluctuations. The quiet magnetosphere (green) spectrum has a power law index near $\alpha \approx -2$. In the Hall current region (black, magenta), a enhancement is observed above $f = f_{ci}$ with power law indices of $\alpha \approx -1$. Heavy dots show the spacecraft spin frequency.

Figure 3. Lower hybrid waves, panel (a), are intense in the Hall current region, where the density scale size (panel b) is small, but quenched where plasma β is large (panel d). Panel c) shows that the electric field fluctuations are polarized perpendicular to the magnetic field.

Figure 4. The measured parallel electric field $E_{\|}$ at the separator boundary (upper panel) is more than 100 times larger than the estimated ηj (lower panel) due to LHDI anomalous resistivity at the edges of the current sheet.

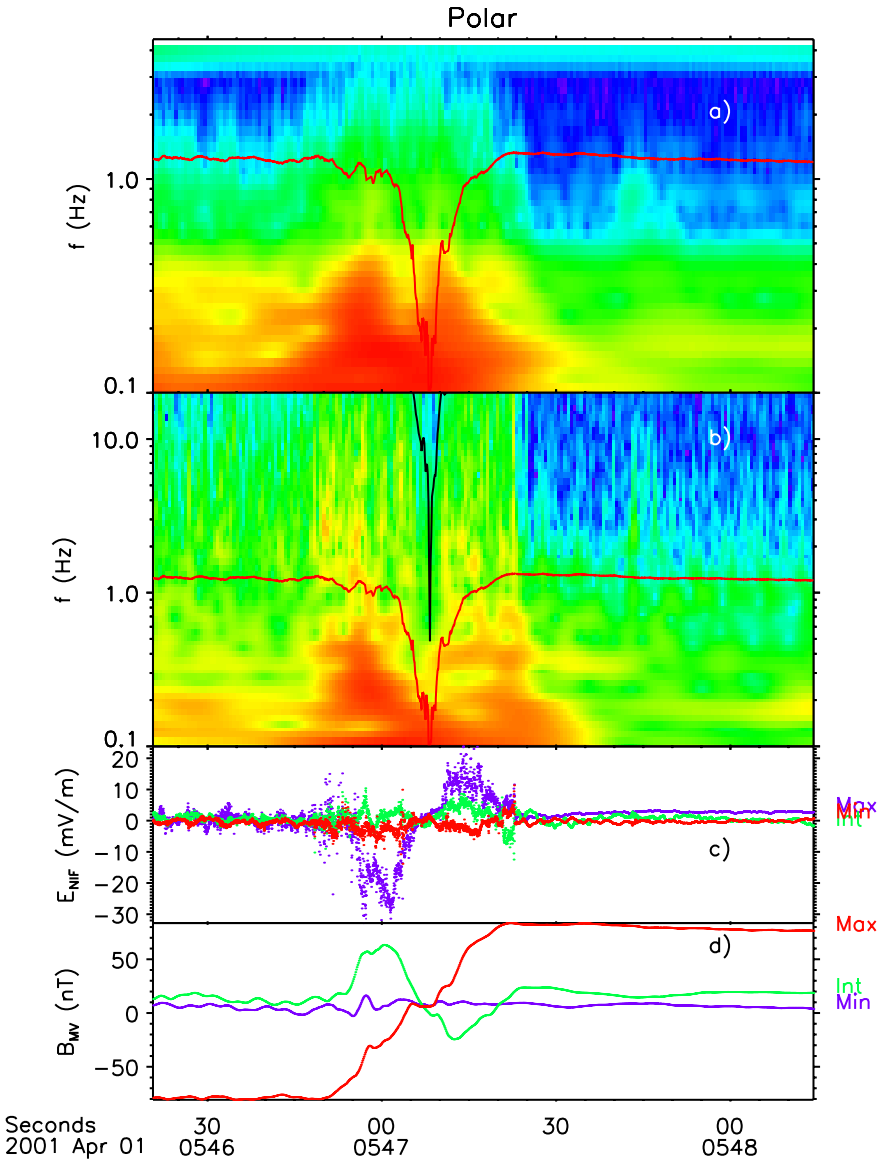
Polar
a)
b)
c)
d)
f (Hz)
1.0
0.1
10.0
f (Hz)
1.0
0.1
20
10
0
−10
−20
−30
E_{NIF} (mV/m)
Max
Int
Min
50
0
−50
B_{MV} (nT)
Max
Int
Min
Seconds
2001 Apr 01
30
0546
00
0547
30
00
0548

Figure 1

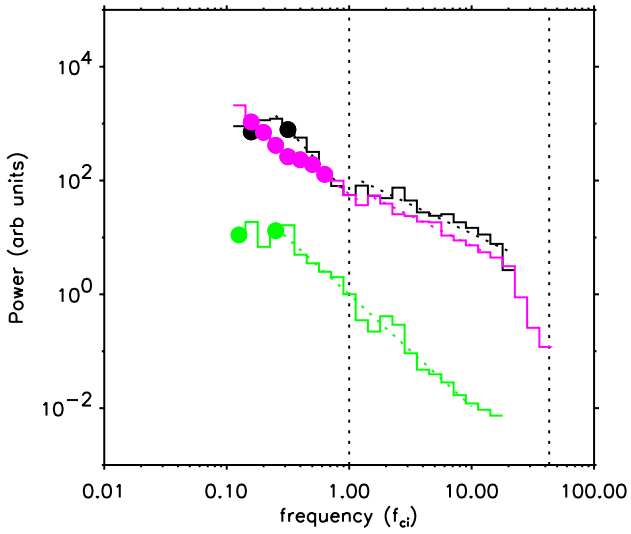
Power (arb units)
10^4
10^2
10^0
10^{-2}
0.01
0.10
1.00
10.00
100.00
frequency (f_{ci})

Figure 2

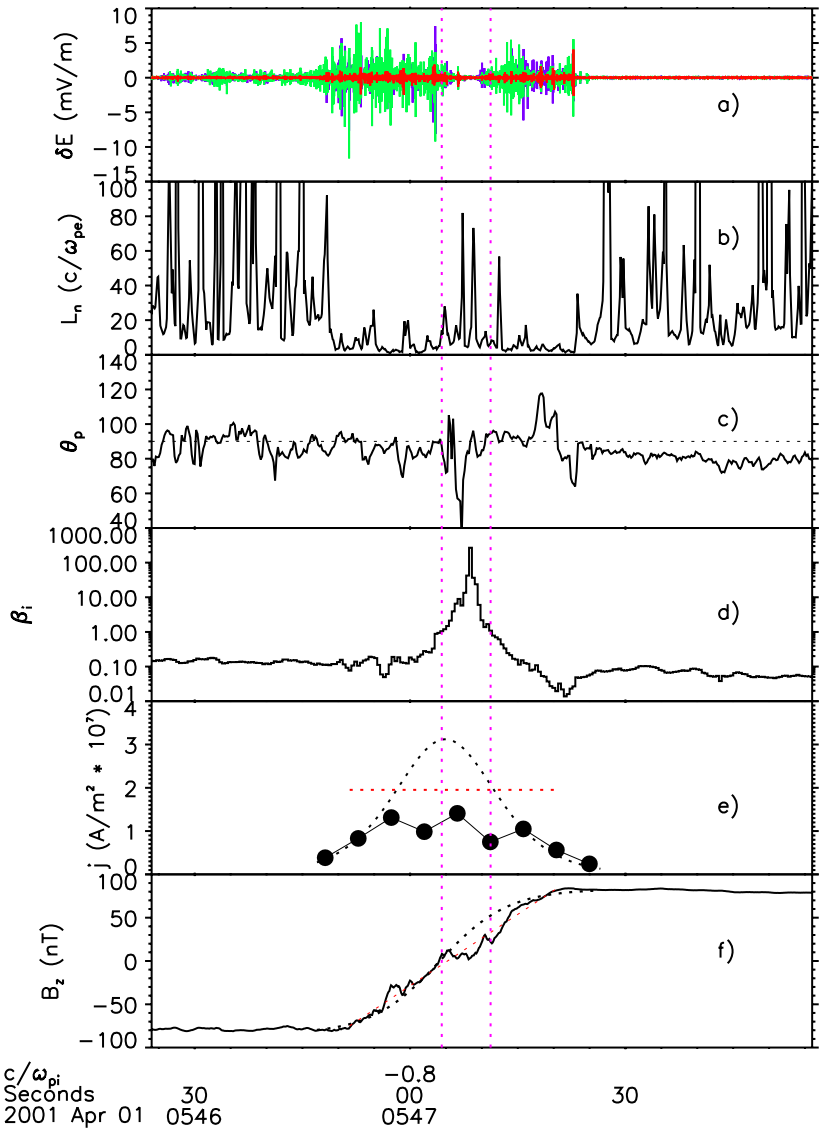
δE (mV/m)
a)
L_n (c/ω_pe)
b)
θ_p
c)
β_i
d)
j (A/m² * 10⁷)
e)
B_z (nT)
f)
c/ω_pi
Seconds
2001 Apr 01
30
0546
−0.8
00
0547
30

Figure 3

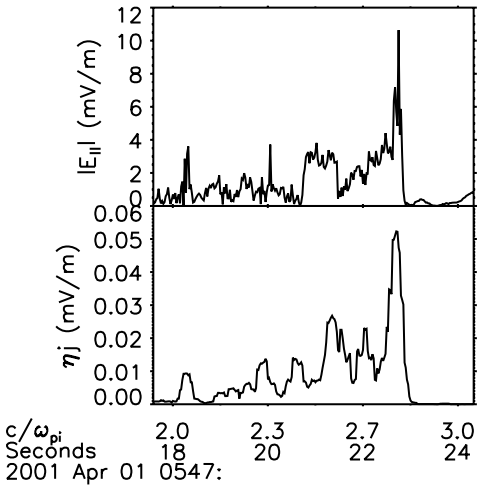
12
10
8
6
4
2
0
$|E_{||}|$ (mV/m)
0.06
0.05
0.04
0.03
0.02
0.01
0.00
ηj (mV/m)
c/ω_{pi} 2.0 2.3 2.7 3.0
Seconds 18 20 22 24
2001 Apr 01 0547:

Figure 4